View metadata, citation and similar papers at core.ac.uk

brought to you by CORE

provided by Edinburgh Research Explorer

THE UNIVERSITY of EDINBURGH

Edinburgh Research Explorer

Force-Extension for DNA in a Nanoslit: Mapping between the 3D and 2D Limits

Citation for published version:
de Haan, HW & Shendruk, TN 2015, 'Force-Extension for DNA in a Nanoslit: Mapping between the 3D and 2D Limits', *ACS MACRO LETTERS*, vol. 4, no. 6, pp. 632-635.
https://doi.org/10.1021/acsmacrolett.5b00138

Digital Object Identifier (DOI):
10.1021/acsmacrolett.5b00138

Link:
Link to publication record in Edinburgh Research Explorer

Document Version:
Peer reviewed version

Published In:
ACS MACRO LETTERS

General rights
Copyright for the publications made accessible via the Edinburgh Research Explorer is retained by the author(s) and / or other copyright owners and it is a condition of accessing these publications that users recognise and abide by the legal requirements associated with these rights.

Take down policy
The University of Edinburgh has made every reasonable effort to ensure that Edinburgh Research Explorer content complies with UK legislation. If you believe that the public display of this file breaches copyright please contact openaccess@ed.ac.uk providing details, and we will remove access to the work immediately and investigate your claim.

Download date: 06. Nov. 2020

Force-Extension for DNA in a Nanoslit: Mapping between the 3D and 2D Limits

Hendrick W. de Haan[*,†] and Tyler N. Shendruk[‡]

University of Ontario Institute of Technology, Faculty of Science, 2000 Simcoe St. North, Oshawa, ON, L1H 7K4, Canada, and The Rudolf Peierls Centre for Theoretical Physics, Department of Physics, Theoretical Physics, University of Oxford, 1 Keble Road, Oxford, OX1 3NP, United Kingdom

E-mail: hendrick.dehaan@uoit.ca

Abstract

The force-extension relation for a semi-flexible polymer confined in a nanoslit is investigated. Both the effective correlation length and force-extension relation change as the chain goes from 3D (large slit heights) to 2D (tight confinement). At low forces, correlations along the polymer give an effective dimensionality. The strong force limit can be interpolated with the weak force limit for two regimes: when confinement dominates over force and vice versa. These interpolations give good agreement with simulations for all slit heights and forces. We thus generalize the Marko-Siggia force-extension relation for DNA and other semi-flexible biopolymers in nanoconfinement.

Many recent studies have focused on static[1–9] and dynamic[10–15] properties of semiflexible biopolymers, such as DNA, within nanoslits,[16,17] nanochannels[18–21] and crowded environments.[22–24] Here, we study polymers of contour length L_C confined within nanoslits and subjected to a stretching force F with resulting extension x. We seek to generalize the Marko-Siggia (MS) force-extension relation (FER) to confined environments. Experimental examples include DNA stretched by electric fields in nanoslits[25] and tug-of-war or nanopit-type devices[26–29]. Both the 3D[30,31] and 2D[32] limits of the FER have been studied extensively but few studies investigate the crossover from 3D to 2D with confinement.[33] While scaling theories quite successfully predict conformations and dynamics of confined macromolecules,[34] a generalization of the FER[35] is needed. Chen *et al.* compared simulations to an FER proposed without derivation.[36] Since x was defined as the distance between the ends in the direction of the force, the low-force regime was unresolved. We apply a force $\vec{F}_1 = F\hat{x}$ (where $\hat{x}$ lies in the plane of the slit) to monomer 1, $\vec{F}_N = -F\hat{x}$ to the last monomer and define $x = (\vec{r}_1 - \vec{r}_N)\cdot\hat{x}$. This ensures that $x \to 0$ as $F \to 0$ permitting exploration of the low-force regime.

We first find an explicit form of the MS-FER in d discrete dimensions without explicit reference to polymer correlation length. We propose that this generalization can be applied to chains confined in nanochannels of height h if a suitable effective dimensionality d_{eff} is identified. For slits where h is sufficiently small $d_{\text{eff}} = 2$, while $d_{\text{eff}} = 3$ when h is large. Intermediate values of d_{eff} represent the impact of confinement on the FER and map between the 2D to 3D limits. Suitable low-force values arise from the confined correlation length, which can be interpolated with theoretical strong-force limits. By considering the competition between confinement and applied force, we derive the FER in two limits: confinement dominated and force dominated. Comparing with the MS-FER in discrete dimensions shows that the generalization

[*]To whom correspondence should be addressed
[†]University of Ontario Institute of Technology
[‡]University of Oxford

can act as a semi-empirical FER with an effective dimensionality d_{eff} that depends on slit height and applied force.

Our results are substantiated by Langevin dynamics simulations of an ideal polymer of 200 monomers with no interactions between non-neighbouring monomers. The method used here follows standard implementations for a semiflexible polymer[37] and is described in detail in the *Supporting Information* (SI).

We now derive a generalized MS-FER for d discrete dimensions. The FER can be approximated as the interpolation between the low- and strong-force limits. At low forces, we use the Kratky-Porod model[38] in d-dimensions, which describes the polymer as an entropic spring with extension $\frac{x}{L_C} = \frac{2}{d}\frac{FL_\xi}{k_B T}$ (see SI). This limit depends on L_ξ, the *correlation length* between tangent vectors. The correlation length is commonly referred to as *persistence length* but, to avoid ambiguity with the *length scale of mechanical rigidity* $L_\kappa = \kappa/k_B T$, we forgo this term. While L_κ is a thermo-material property, L_ξ depends on dimensionality. The two are not strictly equivalent.

In the strong-force limit, we utilize the equipartition theorem in Fourier space to find $\frac{x}{L_c} = 1 - \left(\frac{d-1}{4}\right)\sqrt{\frac{k_B T}{FL_\kappa}}$ (see SI). Interpolating between the limits produces a generalized MS-FER:

$$F = \frac{k_B T}{L_\kappa}\left(\frac{d-1}{4}\right)^2\left[\left(1-\frac{x}{L_c}\right)^{-2} - 1 + \left(\frac{d}{2}\left(\frac{4}{d-1}\right)^2\frac{L_\kappa}{L_\xi} - 2\right)\frac{x}{L_c}\right] \quad (1)$$

which is consistent with 3D[35] and 2D[32,39] forms.

Reasonable agreement with simulations in 3D (indistinguishable from $h = 199$) is obtained for $d = 3$ and $L_\xi = L_\kappa$ (Fig. 1). The slight over-prediction in the 3D limit is a limitation of the simulations (see SI).

The 2D FER is shifted to larger extensions compared to 3D (Fig. 1). Equation 1 fails to agree with the simulations if L_κ is erroneously utilized as L_ξ (appropriate only in 3D). Not only do the coefficients of the MS-FER change but

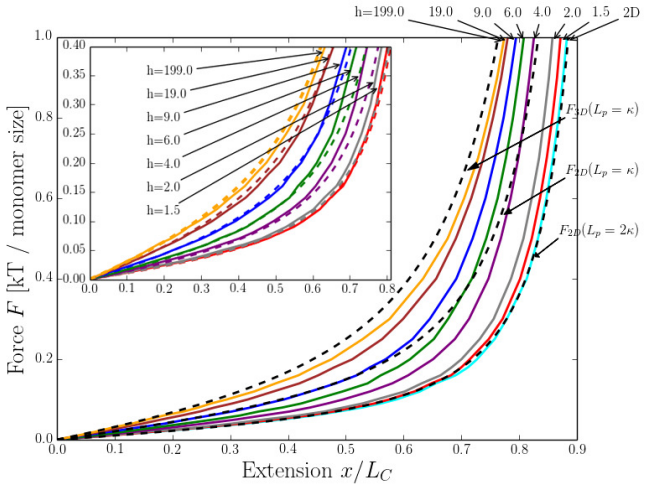

Figure 1: Simulated force-extension relation for various slit heights. Dashed lines indicate theoretical curves (Eqn. 1). In 2D, the curves using both $L_\xi = L_\kappa$ and $L_\xi = 2L_\kappa$ are shown.

$$L_\xi\left(L_\kappa, d\right) = \frac{2L_\kappa}{d-1}, \quad (2)$$

does as well as previously stated[40] and explicitly verified in SI. In 2D, $L_\xi = 2L_\kappa$.

Substituting L_ξ into Eqn. 1 produces the generalized MS-REF without reference to correlation length

$$F\left(x,d\right) = \frac{k_B T}{L_\kappa}\left(\frac{d-1}{4}\right)^2\left[\left(1-\frac{x}{L_c}\right)^{-2} - 1 + 2\left(\frac{d+1}{d-1}\right)\frac{x}{L_c}\right], \quad (3)$$

which is in excellent agreement with both the 3D and 2D limits (Fig. 1).

Equation 3 represents a unified form for discrete dimensions. It also suggests that confinement-induced crossover from 3D to 2D can be discussed in terms of an effective dimensionality $2 \leq d_{\text{eff}} \leq 3$. The polymer does not exist in a fractional dimension but rather a continuous effective dimensionality quantifies the extent to which confinement alters the FER.

We use Eqn. 2 to define the low-force limit to be $d_{\text{eff}} \to d_{\text{eff}}^{\text{low}} = 1 + 2L_\kappa/L_\xi\left(h\right)$. The correlation length is typically measured via $\langle\cos\theta_{i,i+\delta i}\rangle$ for the angle $\theta_{i,i+\delta i}$ between segments i and $i+\delta i$ using $\langle\cos\theta_{i,i+\delta i}\rangle \equiv e^{-\delta i/L_\xi}$. While this approach works well in 2D and 3D, the results for inter-

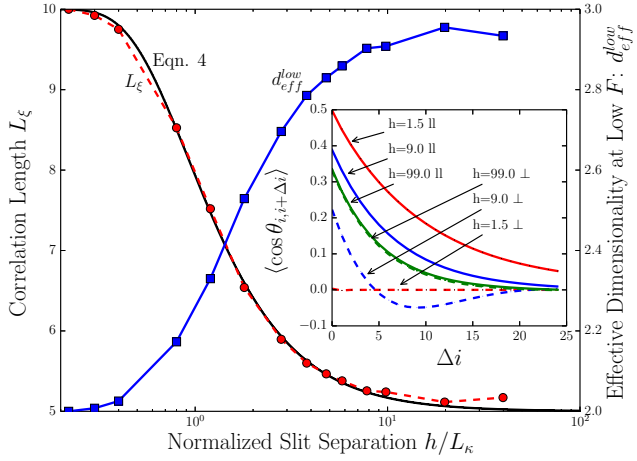

Figure 2: Correlation length (dashed circles) and corresponding effective dimensionality (solid squares) as a function of the slit height. Solid black lines fit the data for $h \leq 2L_\kappa$ (Eqn. 4). Inset shows the components of correlations of direction vectors along the polymer contour.

mediate heights are non-isotropic (Fig. 2; inset). At intermediate heights, the parallel components remain monotonically positive, but the perpendicular component does not. Fully understanding the correlation functions of semiflexible polymers in confinement remains challenging experimentally,[41–44] computationally,[45–47] and analytically.[48–50]

Following Chen *et al.*,[36] we use parallel correlation measurements to define $L_\xi(h)$, which crossesover from 3D to 2D with decreasing slit height (Fig. 2). The black solid line is a fit for $h \leq 2L_\kappa$ given by

$$L_\xi(L_\kappa, h) = L_\kappa \left[2 - e^{-0.88(L_\kappa/h)^{1.41}}\right], \qquad (4)$$

which agrees with theory for both $h \to 0$ and $h \to \infty$. Correspondingly, $d_{\text{eff}}^{\text{low}}(L_\xi/L_\kappa)$ varies smoothly from 3 to 2.

We propose that d_{eff} can be substituted into Eqn. 3 in place of the discrete dimensionality d to produce a semi-empirical FER for confined polymers. For now, we assume d_{eff} is only a function of L_ξ. This allows Eqn. 3 to apply to finite slit confinements as a function of measured L_ξ (Fig. 1; inset).

Good agreement is obtained for moderate extensions. Hence, the d_{eff} approach maps the crossover from 3D to 2D at low forces. However, the theory over-predicts the large-extension regime in comparison to simulations (Fig. 1; inset). This suggests that expressing extension in terms of d_{eff} is only accurate for low-forces

$$\lim_{F \ll \frac{k_BT}{L_\kappa}} \frac{x}{L_c} = \frac{4FL_\kappa}{d_{\text{eff}}^{\text{low}}\left(d_{\text{eff}}^{\text{low}} - 1\right)k_BT}. \qquad (5)$$

Since taut, confined polymers can only accommodate small thermal fluctuations about the line connecting their ends,[51] they feel the effect of the walls less. Hence, confinement effects diminish as force increases causing d^{eff} to increase. Confining walls act to cut off the lowest frequencies allowed in Fourier space, which increases the average extension (see SI). We find the expression for the extension in the strong force limit and arbitrary slit confinement to be

$$\lim_{F \gg \frac{k_BT}{L_\kappa}} \frac{x}{L_c} = 1 - \frac{1}{2}\sqrt{\frac{k_BT}{FL_\kappa}}\left[1 - \frac{1}{\pi}\tan^{-1}\left(c_0 \frac{h}{L_\kappa}\sqrt{\frac{k_BT}{FL_\kappa}}\right)\right] \qquad (6)$$

where c_0 controls the cutoff. This general form for the strong-force FER is in good agreement with the high-force limit of the simulations for all slit heights.

Interpolating between Eqns. 5 and 6 is not possible for arbitrary confinement and we must consider the argument of the arctangent in Eqn. 6. We expand the confinement-dominated $\left(\frac{h}{L_\kappa} \ll \sqrt{\frac{k_BT}{FL_\kappa}}\right)$ and force dominated $\left(\frac{h}{L_\kappa} \gg \sqrt{\frac{k_BT}{FL_\kappa}}\right)$ cases. Interpolation can be found separately in either limit.

Interpolating the force-dominated limit of the strong-force regime with Eqn. 5 gives

$$F = \frac{k_BT}{4L_\kappa}\left[\left(1 - \frac{x}{L_c}\right)^{-2} - 8c_0\frac{L_\kappa}{h}\left(1 - \frac{x}{L_c}\right)^{-1} - \left(1 - 8c_0\frac{L_\kappa}{h}\right) + 2\left\{\frac{d_{\text{eff}}^{\text{low}}\left(d_{\text{eff}}^{\text{low}} - 1\right)}{2} - \left(1 - 4c_0\frac{L_\kappa}{h}\right)\right\}\frac{x}{L_c}\right]. \qquad (7)$$

The cutoff $c_0 = 0.3$ is acceptable and Eqn. 7 is highly accurate at both low and high forces when $h \gtrsim L_\kappa$ (Fig 3). However, the weak confinement approximation breaks down as slit height

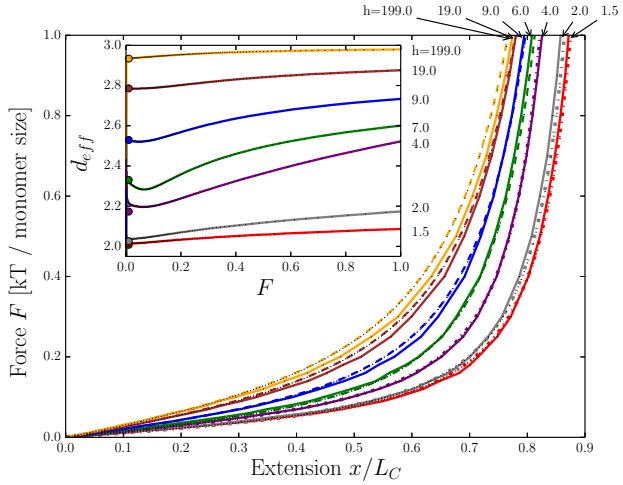

Figure 3: Simulated force extension curves (solid lines) and Eqn. 7 for $h > L_\kappa$ (dashed lines) or Eqn. 8 for $h < L_\kappa$ (dash-dot lines). Inset shows the dependence of effective dimensionality on force for different slit heights Circles indicate $d_{\text{eff}}^{\text{low}}$ values.

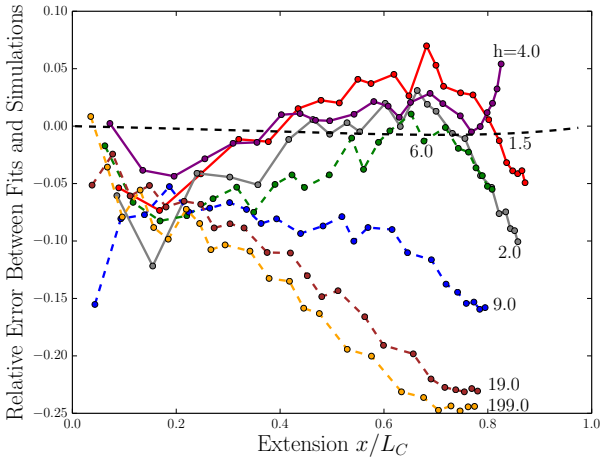

Figure 4: Relative error between simulation results and the interpolation formula given by Eqn. 7 for $h > L_\kappa$ (dashed lines) or Eqn. 8 for $h < L_\kappa$ (solid lines). The dashed black line is the difference between Eqn. 7 at $d_{\text{eff}}^{\text{low}} = 3$ and the 3D Marko-Siggia relation.

decreases.

The other limit of Eqn. 6 is confinement dominated. Interpolating the confinement-dominated limit with Eqn. 5 produces

$$F = \frac{k_B T}{16 L_\kappa}\left[\left(1-\frac{x}{L_c}-\frac{1}{2\pi c_0}\frac{h}{L_\kappa}\right)^{-2}-\left(1+\frac{1}{\pi c_0}\frac{h}{L_\kappa}\right)+2\left(2{d_{\text{eff}}^{\text{low}}}^2-2d_{\text{eff}}^{\text{low}}-1\right)\frac{x}{L_c}\right] \quad (8)$$

where $c_0 = 1.55$ to obtain acceptable agreement. Figure 3 demonstrates that this interpolation is accurate for $h \lesssim L_\kappa$.

The relative error of the interpolations (Eqn. 7 or 8) with the simulations is $(F_{\text{i}}(h,x) - F_{\text{s}}(h,x))/F_{\text{s}}(h,x))$ (Fig. 4). For moderate to tight confinement, the relative error is generally within $\pm$ 5%. Since the results diverge in 3D due to simulation limitations (see SI), the relative error is large for weak confinement. However, the dashed black line is the relative error between the 3D limit of Eqn. 7 and the 3D MS-FER, confirming Eqn. 7 approaches the proper 3D limit.

Having generalized the interpolations for force extension in a slit, we return to the effective dimensionality in Eqn. 3, now recognizing that d_{eff} depends on both slit height and force. We extract $d_{\text{eff}}(F,h)$ by fitting Eqn. 3 to the analytical Eqns. 7 and 8 (Fig. 3; inset). The full d_{eff} shows how the effect of confinement decays with both increasing h and F as the curves move from 2D to 3D. Further, d_{eff} demonstrates quantitatively that the force dependence is dramatic at intermediate heights but otherwise weak.

In conclusion, we have presented a physical picture of the force-extension relation (FER) for DNA confined within nanoslits by introducing an effective dimensionality, d_{eff}. Using d_{eff} in a generalized Marko-Siggia FER leads to good agreement with simulations for all slit heights and forces. At low forces, d_{eff} is determined from in-plane correlations. However, the effect of confinement is reduced for larger forces. Via interpolation, we derived FERs for force-dominated (near 3D) and confinement-dominated (near 2D) systems. These formulas give good agreement with all simulation results. Comparison to the generalized Marko-Siggia yields d_{eff} as a function of both slit height and stretching force. For tight confinements, $d_{\text{eff}} \to 2$ but tends towards 3 as slit height increases. The effective dimensionality thus provides as a useful physical perspective on force-extension curves for biopolymers subject to natural and artificial confinement.

Acknowledgement Simulations performed using HOOMD Blue[52] on SHARCNET (www.sharcnet.ca). The authors gratefully ac-

knowledge useful discussions with Alexander R. Klotz and EMBO funding to T.N.S (ALTF181-2013).

Supporting Information Available: Detailed description of simulation method. Simulations of $N = \{300, 400\}$ at $h = 19.0$ verifying no appreciable difference in the force-extension curves. Mathematical derivations of the correlation length, and the weak- and strong-force limits in d-dimensions and subject to confinement. This material is available free of charge via the Internet at `http://pubs.acs.org/`.

References

(1) Lin, P.-K.; Fu, C.-C.; Chen, Y.-L.; Chen, Y.-R.; Wei, P.-K.; Kuan, C. H.; Fann, W. S. *Phys. Rev. E* **2007**, *76*, 011806.

(2) Dimitrov, D. I.; Milchev, A.; Binder, K.; Klushin, L. I.; Skvortsov, A. M. *The Journal of Chemical Physics* **2008**, *128*.

(3) Cifra, P.; Benková, Z.; Bleha, T. *The Journal of Physical Chemistry B* **2009**, *113*, 1843–1851.

(4) Tang, J.; Trahan, D. W.; Doyle, P. S. *Macromolecules* **2010**, *43*, 3081–3089.

(5) Dai, L.; Jones, J. J.; van der Maarel, J. R. C.; Doyle, P. S. *Soft Matter* **2012**, *8*, 2972–2982.

(6) Cifra, P. *The Journal of Chemical Physics* **2012**, *136*.

(7) Hsu, H.-P.; Binder, K. *Macromolecules* **2013**, *46*, 8017–8025.

(8) Chen, Y.-L.; Lin, Y.-H.; Chang, J.-F.; Lin, P.-k. *Macromolecules* **2014**, *47*, 1199–1205.

(9) Benkova, Z.; Namer, P.; Cifra, P. *Soft Matter* **2015**,

(10) Hsieh, C.-C.; Balducci, A.; Doyle, P. S. *Macromolecules* **2007**, *40*, 5196–5205.

(11) Strychalski, E. A.; Levy, S. L.; Craighead, H. G. *Macromolecules* **2008**, *41*, 7716–7721.

(12) Tang, J.; Levy, S. L.; Trahan, D. W.; Jones, J. J.; Craighead, H. G.; Doyle, P. S. *Macromolecules* **2010**, *43*, 7368–7377.

(13) Milchev, A. *Journal of Physics: Condensed Matter* **2011**, *23*, 103101.

(14) Trahan, D. W.; Doyle, P. S. *Macromolecules* **2011**, *44*, 383–392.

(15) Dai, L.; Tree, D. R.; van der Maarel, J. R. C.; Dorfman, K. D.; Doyle, P. S. *Phys. Rev. Lett.* **2013**, *110*, 168105.

(16) Jo, K.; Dhingra, D. M.; Odijk, T.; de Pablo, J. J.; Graham, M. D.; Runnheim, R.; Forrest, D.; Schwartz, D. C. *Proceedings of the National Academy of Sciences* **2007**, *104*, 2673–2678.

(17) Orlandini, E.; Micheletti, C. *Journal of Biological Physics* **2013**, *39*, 267–275.

(18) Reisner, W.; Morton, K. J.; Riehn, R.; Wang, Y. M.; Yu, Z.; Rosen, M.; Sturm, J. C.; Chou, S. Y.; Frey, E.; Austin, R. H. *Phys. Rev. Lett.* **2005**, *94*, 196101.

(19) Tree, D. R.; Wang, Y.; Dorfman, K. D. *Phys. Rev. Lett.* **2013**, *110*, 208103.

(20) Tree, D. R.; Wang, Y.; Dorfman, K. D. *Biomicrofluidics* **2013**, *7*, 054118.

(21) Vázquez-Montejo, P.; McDargh, Z.; Deserno, M.; Guven, J. *arXiv preprint arXiv:1503.01023* **2015**,

(22) Shin, J.; Cherstvy, A. G.; Metzler, R. *New Journal of Physics* **2014**, *16*, 053047.

(23) Shin, J.; Cherstvy, A. G.; Metzler, R. *ACS Macro Letters* **2015**, *4*, 202–206.

(24) Shendruk, T. N.; Bertrand, M.; de Haan, H. W.; Harden, J. L.; Slater, G. W. *Biophysical Journal* **2015**, *108*, 810 – 820.

(25) K.K. Sriram, Y. L. Y. C., J.W. Yeh; Chou, C. *Nucleic Acids Res.* **2014**, *42*, e85.

(26) Reisner, W.; Larsen, N. B.; Flyvbjerg, H.; Tegenfeldt, J. O.; Kristensen, A. *Proceedings of the National Academy of Sciences* **2009**, *106*, 79–84.

(27) Klotz, A. R.; Brandão, H. B.; Reisner, W. W. *Macromolecules* **2012**, *45*, 2122–2127.

(28) Yeh, J.-W.; Taloni, A.; Chen, Y.-L.; Chou, C.-F. *Nano Letters* **2012**, *12*, 1597–1602.

(29) Kounovsky-Shafer, K. L.; Hernández-Ortiz, J. P.; Jo, K.; Odijk, T.; de Pablo, J. J.; Schwartz, D. C. *Macromolecules* **2013**, *46*, 8356–8368.

(30) Bustamante, C.; Smith, S. B.; Liphardt, J.; Smith, D. *Current Opinion in Structural Biology* **2000**, *10*, 279 – 285.

(31) Bustamante, C.; Bryant, Z.; Smith, S. B. *Nature* **2003**, *421*, 423–427.

(32) Hsu, H.-P.; Paul, W.; Binder, K. *EPL (Europhysics Letters)* **2011**, *95*, 68004.

(33) Taloni, A.; Yeh, J.-W.; Chou, C.-F. *Macromolecules* **2013**, *46*, 7989–8002.

(34) Tree, D. R.; Reinhart, W. F.; Dorfman, K. D. *Macromolecules* **2014**, *47*, 3672–3684.

(35) Marko, J. F.; Siggia, E. D. *Macromolecules* **1995**, *28*, 8759–8770.

(36) Chen, Y.-L.; Lin, P.-k.; Chou, C.-F. *Macromolecules* **2010**, *43*, 10204–10207.

(37) Slater, G. W.; Holm, C.; Chubynsky, M. V.; de Haan, H. W.; Dubé, A.; Grass, K.; Hickey, O. A.; Kingsburry, C.; Sean, D.; Shendruk, T. N.; Zhan, L. *Electrophoresis* **2009**, *30*, 792–818.

(38) Kratky, O.; Porod, G. *Recueil des Travaux Chimiques des Pays-Bas* **1949**, *68*, 1106–1122.

(39) Prasad, A.; Hori, Y.; Kondev, J. *Phys. Rev. E* **2005**, *72*, 041918.

(40) Huang, A.; Adhikari, R.; Bhattacharya, A.; Binder, K. *EPL (Europhysics Letters)* **2014**, *105*, 18002.

(41) Köster, S.; Steinhauser, D.; Pfohl, T. *Journal of Physics: Condensed Matter* **2005**, *17*, S4091.

(42) Köster, S.; Stark, H.; Pfohl, T.; Kierfeld, J. *Biophysical Reviews and Letters* **2007**, *02*, 155–166.

(43) Köster, S.; Kierfeld, J.; Pfohl, T. *The European Physical Journal E* **2008**, *25*, 439–449.

(44) Nöding, B.; Köster, S. *Phys. Rev. Lett.* **2012**, *108*, 088101.

(45) Cifra, P.; Benková, Z.; Bleha, T. *The Journal of Physical Chemistry B* **2008**, *112*, 1367–1375.

(46) Cifra, P.; Benkova, Z.; Bleha, T. *Faraday Discuss.* **2008**, *139*, 377–392.

(47) Benková, Z.; Cifra, P. *Macromolecules* **2012**, *45*, 2597–2608.

(48) Harnau, L.; Reineker, P. *Phys. Rev. E* **1999**, *60*, 4671–4676.

(49) Choi, M. C.; Santangelo, C. D.; Pelletier, O.; Kim, J. H.; Kwon, S. Y.; Wen, Z.; Li, Y.; Pincus, P. A.; Safinya, C. R.; Kim, M. W. *Macromolecules* **2005**, *38*, 9882–9884.

(50) Wagner, F.; Lattanzi, G.; Frey, E. *Phys. Rev. E* **2007**, *75*, 050902.

(51) Baba, T.; Sakaue, T.; Murayama, Y. *Macromolecules* **2012**, *45*, 2857–2862.

(52) Anderson, J. A.; Lorenz, C. D.; Travesset, A. *Journal of Computational Physics* **2008**, *227*, 5342 – 5359.